Design, Fabrication and Experimental Analysis of a 3-D Soft Robotic Snake

Yun Qin[1], Zhenyu Wan[1], Yinan Sun, Erik H. Skorina, Ming Luo, and Cagdas D. Onal

***Abstract*— Snake robots are an emerging approach for navigating complicated and constrained environments. While existing snake robots rely on traditional articulated joints, we have been investigating the use of soft robotic modules which can allow for better compliance with the environment. In this article we present the first soft-material snake robot capable of non-planar locomotion. We performed experiments on the modules that make up the snake robot to determine the ideal material, settling on Ecoflex 0050. Combining 4 modules into the full soft snake, we performed locomotion experiments using both serpentine and sidewinding gaits. We determined that its maximum speed under serpentine locomotion was 131.6 mm/s (0.25 body lengths per second) while under sidewinding it was 65.2 mm/s (0.12 body lengths per second). Finally, we tested these gaits on other surfaces and found that the sidewinding could move more reliably on different surfaces.**

I. Introduction

Robots offer great promise in assisting search-and rescue operations in extremely uncertain and cluttered environments after a variety of accidents. These applications require special robotic capabilities that may not be fulfilled by traditional wheeled robots. Biological snakes provide a good inspiration for designing robots to overcome these challenges. The simple structure of the snake body has the capability to traverse complex, constrained, 3-D environments. Snakes can fit though small gaps, move over rough terrain, and climb shear inclines, tasks that would help them in navigating dense undergrowth of a forest or the wreckage of a collapsed building.

Snake robots have been developed using traditional robotic structures composed of rigid links and discrete joints. Wright et al. developed a simple, modular snake robot made of servo motors mounted in series, capable of climbing up the inside of a pipe [1]. Crespi et al. developed a larger, more complex snake robot with DC motors and detachable wheels capable of locomotion on land and in water [2]. Snake robots can use different methods of locomotion, including most frequently serpentine locomotion (or lateral undulation) and sidewinding locomotion [3]–[6].

[1] Yun Qin and Zhenyu Wan contributed equally to this work.

The authors are with the Mechanical Engineering Department and Robotics Engineering Program, Worcester Polytechnic Institute, MA 01609, USA. All correspondence should be addressed to Cagdas D. Onal cdonal@wpi.edu

This material is based upon work supported by the National Science Foundation under grant numbers IIS-1551219 and CMMI-1728412. Any opinions, findings, and conclusions or recommendations expressed in this material are those of the authors and do not necessarily reflect the views of the National Science Foundation.

Digital Object Identifier (DOI): see top of this page.

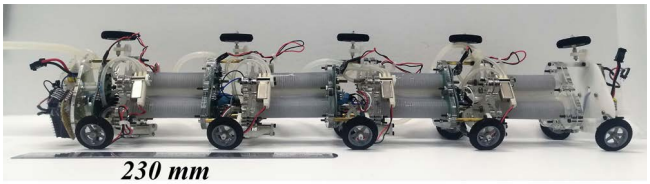

Fig. 1. The 3-D Soft Snake Robot. The body length of the SRS is 530 mm, and the height is 100 mm. The length of each module is 100mm, which is made up of 70 mm of bending segment and connectors.

Rigid robotic snakes, though capable of snake-like motion [7], [8], suffer from a number of problems. The fact that rigid snakes only articulate at discrete points mean that they can only approximate the smooth continuum body motions of biological snakes. To address this problem, we have focused on developing soft pressure-operated robotic snakes [9], [10] which use pneumatic pressure to actuate silicone rubber 1-degree of freedom (DoF) bending segments, resulting in a constant-curvature deformation along the length of each segment. Like other soft robots benefits [11]–[13],this results in a flexible, safe, and adaptive motion, effectively reproducing the lateral undulation gait of a biological snake on a 2-D plane.

While planar bending is all that is required to generate serpentine locomotion, it is insufficient for the more complex environments that represent the desired use-case for this system. Real-world environments include surfaces with different properties as well as steps that planar snake robots can find difficult or impossible to traverse.

In this paper we introduce a modular soft robotic snake (SRS) (shown in Fig. 1) capable of three dimensional gaits: a so-called ”3-D” Snake Robot. We tested two different gaits used by biological snakes using this SRS. Each module of this snake is actuated using reverse Pneumatic Artificial Muscles (rPAMs) [14], which are tubes of silicone rubber wrapped in thread that extend when pressurized. With three rPAMs, each module has 3 bending degrees-of-freedom (DoF), but we mainly use 2-DOF in our experiments, since the extension along the vertical direction is unnecessary. This allows it to lift itself off the ground and perform sidewinding gaits for motion over more difficult terrain.

This work represents:

- The first 3-D soft-material robotic snake
- The assessment of 3-D soft-material snake on various common terrains

II. Snake Design

A. Module Design and Fabrication

To make the snake easier to repair, and make the structure of the snake more versatile, we constructed the SRS out of a series of modules. Previous prototypes we have constructed have suffered when a failure in a single bending segment required the replacement of the entire body [10]. For this SRS, a faulty module could be easily switched out, increasing the reliability of the system. In addition, the modualarity of the SRS allows us to scale the number of segments and DoF at will. This can allow us to easily test the behavior of the SRS under conditions with different modules.

Each module includes a soft bending segment constructed from 3 rPAM actuators, the three valves used to control the air flow in this segment, and a slave controller circuit to drive these valves. The states of the valves on each module are controlled by a main controller, which is connected to each slave controller by I2C communication. The rPAM actuators consist of tubes of silicone rubber wrapped in helix of thread. When pressurized, the shallow angle of the thread (approaching perpendicular to the tube) prevents the tube from deforming radially into a sphere, and instead causes it to extend.

Three of these rPAM actuators are fused together with silicone to form a soft bending segment. When one of the actuators in a segment is pressurized, the un-actuated material causes it to bend in the opposite direction.

Each chamber is sealed at both ends using a pair of acrylic plates bolted together around a flange of silicone, so the flange of silicone can be seen as a gasket. [15] A vent screw (A screw with a hole drilled through it) is used on one side of each chamber to provide access for pneumatic pressure. Tubes connect each chamber to a corresponding valve. Each of these valves is given commands by the custom slave controller board mounted on one end of the module (replacing one of the acrylic plates). The fabrication steps are shown in Fig.2.

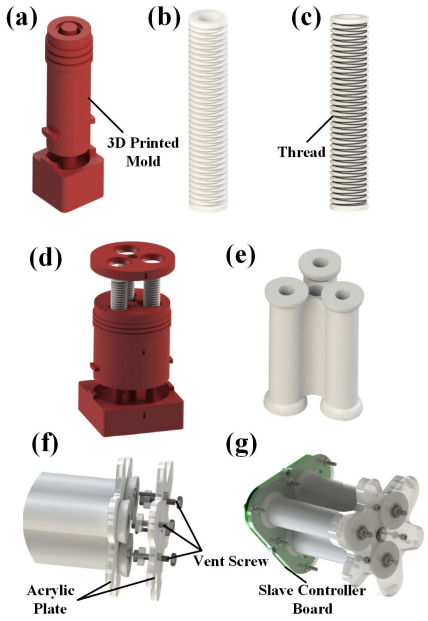

Fig. 2. Fabrication process of the 3-D soft robotic bending module. (a) The mold of a single rPAM. (b) The single actuator without thread. (c) The threaded single actuator. (d) The mold of the outer body, which is used to combine the three threaded single actuators. (e) The demolded soft 3-D bending segment. (f) The soft segment sealed with acrylic plates and the vent screw. (g) The assembled soft robotic bending module.

B. Single Module Verification

We created modules using several different varieties of silicone rubber: Smooth-on Ecoflex 0030, Ecoflex 0050, and DragonSkin 10, each with different material properties. This would allow us to examine the behavior of the modules, as well determine which material the SRS as a whole should be constructed from. We applied constant pressures to the modules, and recorded the resulting motion using an OptiTrack motion capture system as shown in Figure 3. Because of the significant differences in the material properties of the three silicone rubbers, different pressures were used for different materials. We used 8 psi (55.16 kPa) as the maximum pressure for Ecoflex 0030, and 14 psi (96.53 kPa) for Ecoflex 0050, since such pressure can fully show their bending property without bursting. We used 25 Psi (172.37 kPa) for DragonSkin 10, which was the maximum our system could effectively output. Thus, for each module, we tested 4 different pressures based on the maximum pressure to explore the effect of pressure. The results of these experiments can be seen in Figure 4. From these experiments we can confirm that the modules were well-constructed, exhibiting similar behavior in all three directions of actuation, especially when the pressure is high.

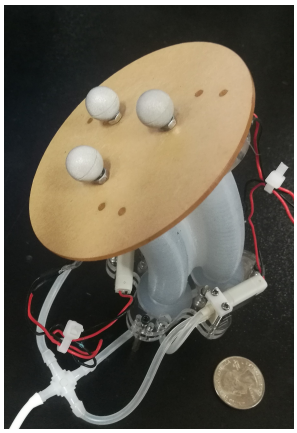

Fig. 3. A representative image from single module experiments. The three motion tracking markers fixed are used to record the bending angles. The diameter of the chamber is 8mm, while the diameter of the entire bending segment is 15.5mm.

From Figure 4.(c) we can see that DragonSkin 10 has a much smaller maximum bending angle than the other two. While it is stronger and more durable, this lack of bending at the available pressures makes it unsuitable for this version of the SRS. Ecoflex 0030 and Ecoflex 0050

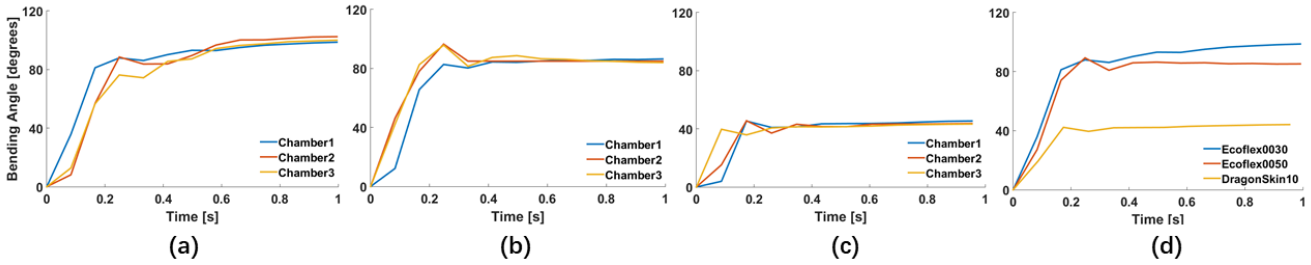

Fig. 4. The results step-response tests on modules of different materials. Each test was performed at the maximum possible pressure, comparing the three chambers of a single module (a-c). a) DragonSkin 10 at 25 psi (172.37 kPa), b) Ecoflex 0050 at 14 psi (96.53 kPa), c) Ecoflex 0030 at 8 psi (55.16 kPa), d) Maximum bending angle of each module of different material (from a-c)

have similar maximum bending angles. However, Ecoflex 0050 can withstand more force and be more reliable than its softer counterpart. Hence modules made out of Ecoflex 0050 would be able to function better and more reliably while carrying all the hardware components of the SRS. Thus, we chose Ecoflex 0050 to be the material used for our 3-D Soft Snake Robot.

C. Full System Composition

The full system was composed of 4 of these soft bending modules mounted in series. The modules were connected together using screws and spacers. The gap between soft modules provided enough space for wires, tubes and passive wheels. Undulatory snake locomotion requires that the snake have much higher friction in the normal direction (perpendicular to the body of the snake) than in the tangential direction. Passive wheels are a simple solution commonly used in the literature for this purpose. The passive wheels on each module were connected using a wheel holder made out of acrylic plates, the aim of using three passive wheels was to allow our 3-D SRS to be capable of lateral undulation at every orientation [9], [10].

We mounted the master control board at the head of the SRS. The mater controller is an Arduino pro mini with an atmeg328 chip on it. It communicates via I2C to the four slave controllers each mounted on a module. To power the master control board, slave boards, and the valves, we mounted an 8 V battery to the head and the tail. Finally, in order keep the head and the tail similar weights, we added a 150 g mass at the tail. This served to keep the snake symmetric, and keep the tail pressing against the ground.

III. Control Schemes

With no feedback, the SRS performs low level open-loop control The master controller determines the frequency, offset and other parameters for a given gait, and the slave controllers execute it by driving the valves. The aim of this snake robot is to study two different gaits used by biological snakes: lateral undulation (serpentine) and side-winding.

A. Lateral Undulation

Serpentine locomotion represents the classic snake motion. The snake creates a horizontal traveling wave down its body, and uses the anisotropic friction of its underside to propel itself forward. For serpentine locomotion, we only actuate the lower two chambers on each module, bending them to the right and to the left. The equation we use for this traveling wave is as follows [16]:

$$K_i = \alpha sin(\omega t + i\beta) + \phi \qquad i \in (0, 1, 2, ..., N-1) \quad (1)$$

for the desired trajectory of each module, where ω is the frequency of the movement, β is the phase difference between each module, α is the bending amplitude for the segments under a given air pressure, ϕ is the offset which can be used for steering, and K_i is the state of the ith segment. While $K_i > 0$ the segment is actuated in one direction, while if $K_i < 0$ the segment is actuated in the other direction. We fix ϕ at zero for all the gaits studied in this paper and α is directly controlled by the air pressure level.

B. Sidewinding

Sidewinding locomotion is a type of snake locomotion that involves the snake lifting its body off the ground. It combines lifting and lowering itself with undulation in such a way that when part of its body is moving a certain direction it is in contact with the ground, while when part of its body is moving in the opposite direction it is always in the air. Together, the parts of the body in contact with the ground serve to push the snake in a constant direction [17]. This gait allows a snake to avoid the frictional losses associated with serpentine locomotion, making it highly efficient.

In order to implement this gait on the SRS, we combined the horizontal traveling wave of the serpentine gait with a vertical wave of the same frequency.

$$K_{ih} = \alpha sin(\omega t + i\beta) + \phi \qquad i \in (0, 1, 2, ..., N-1) \quad (2)$$

$$K_{iv} = \alpha sin(\omega t + i\beta + \frac{\pi}{2}) + \phi \qquad i \in (0, 1, 2, ..., N-1) \quad (3)$$

The state of the ith segment is showed by K_{ih} and K_{iv} in each direction respectively. The two waves share the same frequency ω , bending amplitude α and phase difference between modules β, the distinction between the wave is that they operate in different planes which are orthogonal.

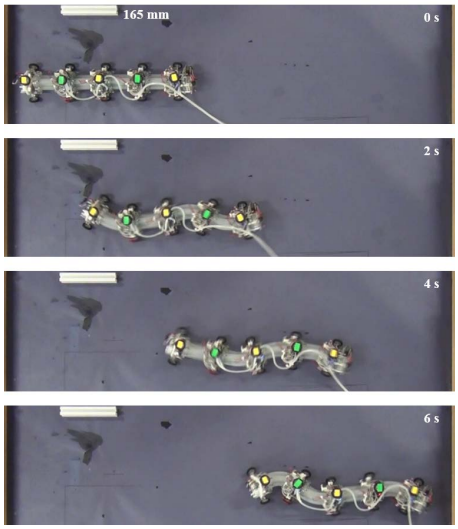

Fig. 5. Example frames from a serpentine locomotion experiment. Note the green and yellow trackers which were used to track the position of the snake.

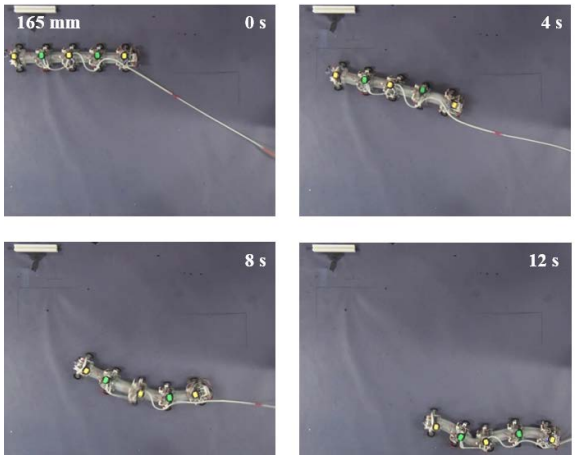

Fig. 6. Example frames from a sidewinding locomotion experiment. Note the green and yellow trackers which were used to track the snake.

This results in each actuator inscribing a circle, with the phase of each segment offset from the ones before and after it. For ease of implementation, we approximated the circular motion for each actuator as hexagonal motion using only low-frequency binary states for each actuator. As with serpentine locomotion, we could adjust the offset β and the frequency ω to tune the gait performance.

IV. Experimental Results

We performed experiments testing the behavior of the snake robot following both gaits with varying parameters and on 3 different surfaces. We mounted markers on the end of each segment, and recorded video from above as the snake moved. Example frames can be seen in Figure 5 for the serpentine locomotion and Figure 6 for the sidewinding locomotion. From the video, we calculated the position of each marker, and averaged them to calculate the centeroid

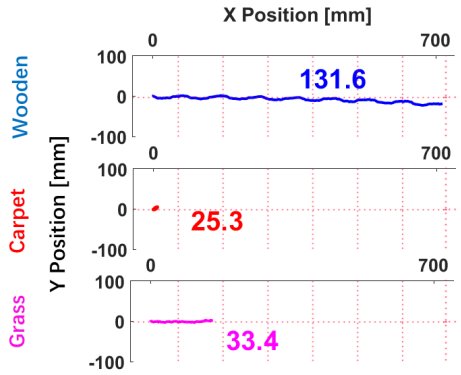

Fig. 8. The results of serpentine locomotion experiments on different surfaces with frequency = 1.5 Hz and offset β = 150. Trajectories are shown for each surface with the corresponding average speed in mm/s.

position of the snake. We used the average speed of the snake center to gauge the gait's performance. We tested a range of control parameters for each gait type on a flat wooden benchtop, allowing us to determine the maximum performance of the each type.

In addition, we compared the performance of one set of gait parameters for each locomotion type on different surfaces. In addition to the flat wooden surface, we tested the snake on carpet (Home Depot Viking 7 mm tall) and artificial grass (Ecomatrix 3 cm tall) to evaluate the performance of our soft robotic snake in both indoor and outdoor scenarios.

A. Serpentine

When testing the behavior of the snake using serpentine locomotion, we used the following control parameters: Frequency $f = \frac{\omega}{2\pi}$ = 1.5, 1.75, and 2 Hz and phase difference β = 60, 90, 120, and 150. The results of these experiments can be seen in Figure 7. From these results, we can see that maximum average speed of the Snake is 131.6 mm/s and is achieved at β = 150 and ω = 1.5 Hz. This represents a maximum velocity of 0.25 body-lengths per second.

During serpentine locomotion experiments, we observed that the actuation of the lower actuators caused the SRS segments to lift slightly up as they bent sideways. This resulted in a lighter contact between the snake and the ground. This in turn probably resulted in slower serpentine locomotion compared to our earlier 2-D prototypes [10], as the frictional anisotropy of the passive wheels played less of a role.

Using these parameters, we tested the undulation performance of the snake on carpet and artificial grass. The results of these experiments can be seen in Figure 8.

While the average speed of the serpentine locomotion on carpet was 25.3 mm/s, the snake moved very little during the experiment. This is because its center of gravity shifted around rapidly and in random directions that cannot provide enough force for heading foward. By contrast, the serpentine locomotion achieved an average speed of 33.4 mm/s on artificial grass. While this is slower than on the flat surface,

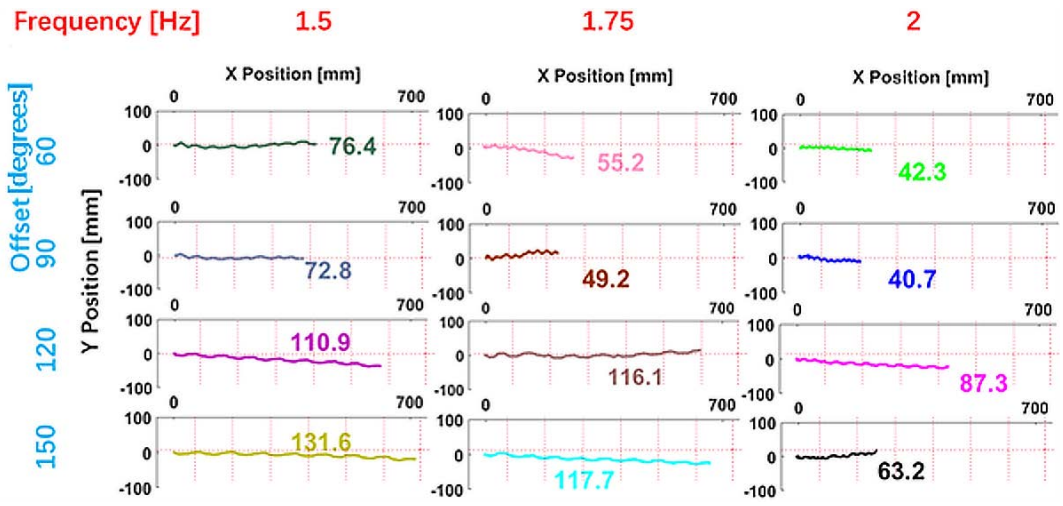

Fig. 7. The results of serpentine locomotion experiments on a flat wooden benchtop under different control parameters. Shown are the trajectories for each combination of control parameters with the associated average speed in mm/s.

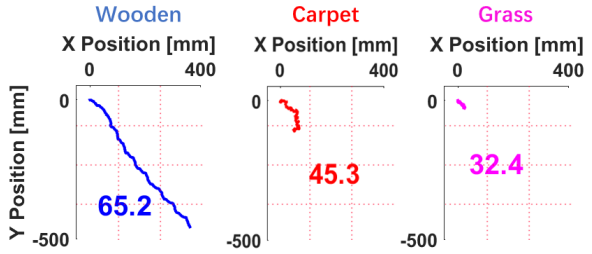

Fig. 10. The results of sidewinding locomotion experiments on different surfaces with frequency = 1.5 Hz and offset β = 120. Trajectories are shown for each surface with the corresponding average speed in mm/s.

it is still a usable velocity, demonstrating the snake's ability to move on other surfaces.

B. Sidewinding

We also tested the behavior of the snake using sidewinding locomotion with Frequency $f = \frac{\omega}{2\pi}$ = 1.5, 1.75, and 2 Hz and phase difference β = 30, 60, 90, 120, and 150. The results of these experiments can be seen in Figure 9. From these results we can see that the sidewinding gait is fastest with a phase difference of 120 and a frequency of 1.5 Hz. At 65.2 mm/s, this is just over 0.12 body-lengths per second, and is about half the speed of the serpentine locomotion. This maximum velocity occurs at similar dynamic parameters to those of the serpentine locomotion, suggesting that this area in the parameter space interacts well with the dynamic properties of the 3-D SRS.

We tested the performance of this gait on the other 2 surfaces, the results of which can be seen in Figure 10. From this, we can see while the performance of sidewinding on grass was comparable to that of undulation, sidewinding on carpet was significantly faster than undulation. This shows that sidewinding is a more reliable locomotion method on different terrain types, even if it has a lower maximum speed.

V. Conclusion

This article introduced the WPI 3-D soft robotic snake (SRS), a soft-material robotic snake capable of non-planar motion. We employed modular design and fabrication, constructing the SRS out of distinct integrated modules that can be combined and separated as necessary. Each module consists of 3 reverse Pneumatic Artificial Muscles (rPAMs) molded together to form a 2 degree-of-freedom bending segment. When pressurized, each rPAM will result in the segment bending in the opposite direction.

We investigated the behavior of soft robotic modules, and determined that the ideal soft material for our 3-D SRS was Smooth-on Ecoflex 0050. We constructed a full 4-module SRS, and performed experiments using undulation and sidewinding gaits. We investigated a range of control parameters for both gaits and found the ones that resulted in maximum speed for each gait type, 131.6 mm/s for serpentine locomotion and 65.2 mm/s for sidewinding. We tested these gaits on carpet and artificial grass, and found that sidewinding was more effective on these more difficult terrain types.

One problem that we ran into during the design and fabrication of the SRS was buckling. When the pressure in one of the module chambers is too high, the module can twist instead of bending. This behavior was one of the reasons why we used Ecoflex 0050 instead of 0030: the stronger material allowed for comparable bending angles with fewer instances of buckling.

In this article we determined the optimal control parameters for both gaits on a flat wooden benchtop surface, and then tested them on carpet and artificial grass. While the results were promising, highlighting the advantages of the 3-D snake design, they do not represent an exhaustive analysis of the behavior of our snake on multiple terrains. It is possible that different sets of locomotion parameters will produce superior performance. In future work, we

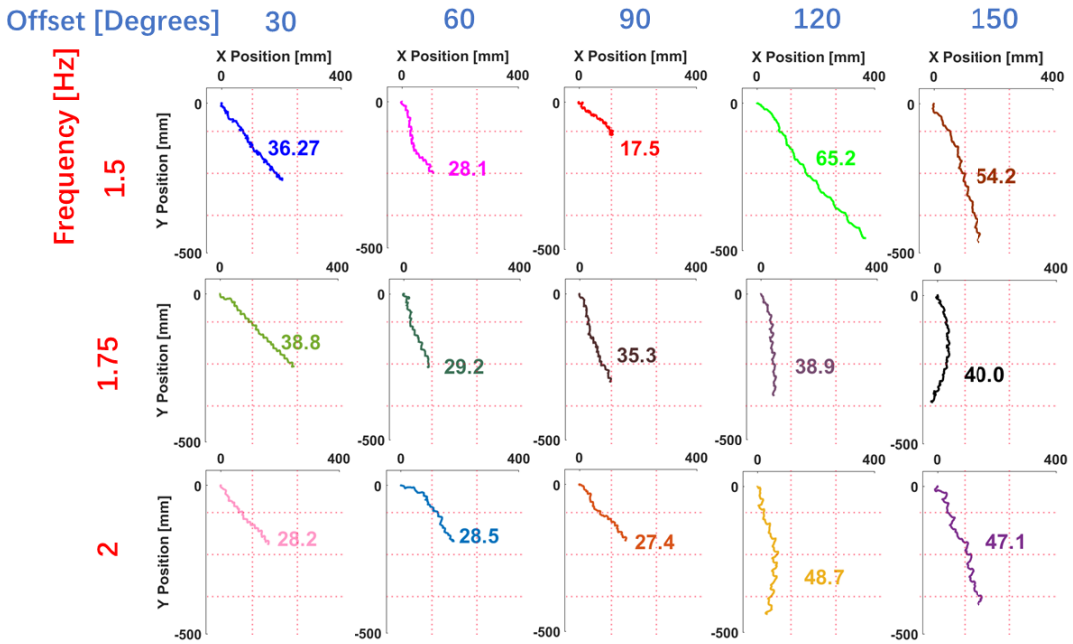

Fig. 9. The results of sidewinding locomotion experiments on a smooth surface under different control parameters. Shown are the trajectories for each combination of control parameters with the associated average speed in mm/s.

would like to investigate alternative parameters, as well as a method for the snake robot to change its control strategy on-the-fly in response to changing conditions. This could include switching between gaits entirely.

Finally, while the sidewinding showed the usefulness of the 3D snake on different terrains, there are other aspects of search-and-rescue scenarios we plan to investigate. These include the snake's ability to traverse steps, climb inclines, and fit through small openings.

References

[1] C. Wright, A. Johnson, A. Peck, Z. McCord, A. Naaktgeboren, P. Gianfortoni, M. Gonzalez-Rivero, R. Hatton, and H. Choset, "Design of a modular snake robot," in *Intelligent Robots and Systems, 2007. IROS 2007. IEEE/RSJ International Conference on*, pp. 2609–2614, IEEE, 2007.

[2] A. Crespi and A. J. Ijspeert, "Amphibot ii: An amphibious snake robot that crawls and swims using a central pattern generator," in *Proceedings of the 9th international conference on climbing and walking robots (CLAWAR 2006)*, no. BIOROB-CONF-2006-001, pp. 19–27, 2006.

[3] S. Hirose and M. Mori, "Biologically inspired snake-like robots," in *Robotics and Biomimetics, 2004. ROBIO 2004. IEEE International Conference on*, pp. 1–7, IEEE, 2004.

[4] F. Matsuno and K. Suenaga, "Control of redundant 3d snake robot based on kinematic model," in *Robotics and Automation, 2003. Proceedings. ICRA'03. IEEE International Conference on*, vol. 2, pp. 2061–2066, IEEE, 2003.

[5] K. L. Paap, T. Christaller, and F. Kirchner, "A robot snake to inspect broken buildings," in *Intelligent Robots and Systems, 2000.(IROS 2000). Proceedings. 2000 IEEE/RSJ International Conference on*, vol. 3, pp. 2079–2082, IEEE, 2000.

[6] Z. Bing, L. Cheng, G. Chen, F. Röhrbein, K. Huang, and A. Knoll, "Towards autonomous locomotion: Cpg-based control of smooth 3d slithering gait transition of a snake-like robot," *Bioinspiration & Biomimetics*, vol. 12, no. 3, p. 035001, 2017.

[7] P. Liljebäck, K. Y. Pettersen, O. Stavdahl, and J. T. Gravdahl, *Snake robots: modelling, mechatronics, and control*. Springer Science & Business Media, 2012.

[8] S. Ma, N. Tadokoro, B. Li, and K. Inoue, "Analysis of creeping locomotion of a snake robot on a slope," in *Robotics and Automation, 2003. Proceedings. ICRA'03. IEEE International Conference on*, vol. 2, pp. 2073–2078, IEEE, 2003.

[9] C. Onal and D. Rus, "Autonomous undulatory serpentine locomotion utilizing body dynamics of a fluidic soft robot," *Bioinspiration and Biomimetics*, vol. 8, no. 2, 2013.

[10] M. Luo, Y. Pan, E. Skorina, W. Tao, F. Chen, S. Ozel, and C. Onal, "Slithering towards autonomy: a self-contained soft robotic snake platform with integrated curvature sensing.," *Bioinspiration & biomimetics*, vol. 10, no. 5, pp. 055001–055001, 2015.

[11] R. F. Shepherd, F. Ilievski, W. Choi, S. A. Morin, A. A. Stokes, A. D. Mazzeo, X. Chen, M. Wang, and G. M. Whitesides, "Multigait soft robot," *Proceedings of the national academy of sciences*, vol. 108, no. 51, pp. 20400–20403, 2011.

[12] C. Laschi and M. Cianchetti, "Soft robotics: new perspectives for robot bodyware and control," *Frontiers in bioengineering and biotechnology*, vol. 2, p. 3, 2014.

[13] S. Kim, C. Laschi, and B. Trimmer, "Soft robotics: a bioinspired evolution in robotics," *Trends in biotechnology*, vol. 31, no. 5, pp. 287–294, 2013.

[14] M. Luo, E. H. Skorina, W. Tao, F. Chen, and C. D. Onal, "Optimized design of a rigid kinematic module for antagonistic soft actuation," in *Technologies for Practical Robot Applications (TePRA), 2015 IEEE International Conference on*, pp. 1–6, IEEE, 2015.

[15] M. Luo, E. Skorina, W. Tao, F. Chen, S. Ozel, Y. Sun, and C. Onal, "Toward modular soft robotics: Proprioceptive curvature sensing and sliding-mode control of soft bidirectional bending modules," *Soft Robotics*, 2017.

[16] M. Luo, M. Agheli, and C. D. Onal, "Theoretical modeling and experimental analysis of a pressure-operated soft robotic snake," *Soft Robotics*, vol. 1, no. 2, pp. 136–146, 2014.

[17] S. Secor, B. Jayne, and A. Bennett, "Locomotor performance and energetic cost of sidewinding by the snake crotalus cerastes," *Journal of Experimental Biology*, vol. 163, no. 1, pp. 1–14, 1992.